


RESEARCH ARTICLE

Amisulpride and L-DOPA modulate subcortical brain nuclei connectivity in resting-state pharmacologic magnetic resonance imaging

Oliver Grimm  | Vera Kopfer | Lea Küpper-Tetzel | Vera Deppert |
Magdalena Kuhn | Moritz de Greck | Andreas Reif

Department of Psychiatry, Psychosomatic
Medicine and Psychotherapy, University
Hospital, Goethe University, Frankfurt,
Germany

Correspondence

Oliver Grimm, Department of Psychiatry,
Psychosomatic Medicine and Psychotherapy,
University Hospital, Goethe University,
Frankfurt, Germany.
Email: oliver.grimm@kgu.de

Funding information

Horizon 2020 Framework Programme, Grant/
Award Number: 667302

Abstract

The precise understanding of the dopaminergic (DA) system and its pharmacological modifications is crucial for diagnosis and treatment of neuropsychiatric disorders, as well as for understanding basic processes, such as motivation and reward. We probed the functional connectivity (FC) of subcortical nuclei related to the DA system according to seed regions defined according to an atlas of subcortical nuclei. We conducted a large pharmacofMRI study using a double-blind, placebo-controlled design, where we examined the effect of L-DOPA, a dopamine precursor, and amisulpride, a D2/D3-receptor antagonist on resting-state FC in 45 healthy young adults using a cross-over design. We examined the FC of subcortical nuclei with connection to the reward system and their reaction to opposing pharmacological probing. Amisulpride increased FC from the putamen to the precuneus and from ventral striatum to precentral gyrus. L-DOPA increased FC from the ventral tegmental area (VTA) to the insula/operculum and between ventral striatum and ventrolateral prefrontal cortex and it disrupted ventral striatal and dorsal caudate FC with the medial prefrontal cortex. In an exploratory analysis, we demonstrated that higher self-rated impulsivity goes together with a significant increase in VTA-mid-cingulate gyrus FC during L-DOPA-challenge. Therefore, our DA challenge modulated distinct large-scale subcortical connectivity networks. A dopamine-boost can increase midbrain DA nuclei connectivity to the cortex. The involvement of the VTA-cingulum connectivity in dependence of impulsivity has implications for diagnosis and therapy in disorders like ADHD.

KEYWORDS

amisulpride, dopamine, insula, L-DOPA, pharmacofMRI, resting-state fMRI, ventral tegmental area

This is an open access article under the terms of the Creative Commons Attribution-NonCommercial-NoDerivs License, which permits use and distribution in any medium, provided the original work is properly cited, the use is non-commercial and no modifications or adaptations are made.

© 2019 The Authors. *Human Brain Mapping* published by Wiley Periodicals, Inc.

1 | INTRODUCTION

Dopaminergic (DA) neurotransmission plays a major role in reward regulation, decision making, executive functioning and action selection of planned movements (Mobbs, Trimmer, Blumstein, & Dayan, 2018) and, via these domains, is crucially involved in a number of neuropsychiatric disorders such as ADHD, substance-use and mood disorders, schizophrenia, and Parkinson's disease. The dopamine (DA) system is modulated in a phasic or tonic way and its spiking is basically a prediction algorithm for future rewards (Schultz, 2015). While animal models and neurophysiologic single cell clamps give good insight into how temporal prediction of reward works, characterization of long-range connectivity in humans is still incomplete, despite some smaller fMRI studies (Di Martino et al., 2008; Honey et al., 2009). The prediction of functional connectivity (FC) during changes of dopamine neuromodulation is not trivial. While there are some computational simulations of DA effects of the frontal cortex (Hass, 2011), we are in urgent need of more experimental data to delineate the brain areas under DA modulation (Lak, Stauffer, & Schultz, 2014). Only by characterizing the exact mechanism of these long-range connectivity patterns of the DA-system, starting from DA nuclei in the midbrain can we understand all features of neuropsychiatric disorders ranging from Lewy-body-dementia to Tourette, schizophrenia, addiction or ADHD (Faraone, 2018; Howes & Kapur, 2009; Whitton, Treadway, & Pizzagalli, 2015).

However, previous explanatory models for the role of DA in ADHD are contradictory. For example, in ADHD both an increase and a decrease in striatal activation during reward anticipation were found (Hägele et al., 2015; Plichta & Scheres, 2014). The direction of the reported changes seems to be dependent on specific paradigms, for example, a de- or increase in a monetary incentive delay task was reported (Ströhle et al., 2008; Von Rhein et al., 2015); decreases were reported by Rubia et al. using a temporal discounting (Rubia, Halari, Christakou, & Taylor, 2009) and rewarded continuous performance task (Rubia et al., 2009). In ADHD, these different deficits were conceptualized as belonging to a "cold" cognitive, inhibitory, and attentive network versus a "hot" paralimbic network regulating motivation and affect (Rubia, 2011). Therefore, more detailed characterization of the DA system is urgently required. Here, we hypothesized that activation or blockade of DA would show differential effects between a "hot" limbic system striatal network in contrast to a "cold" part connected with brain areas involved in executive functioning.

To experimentally test this hypothesis, we manipulated the DA system in two opposing ways in healthy volunteers, by pharmacological means, and conducted neuroimaging thereafter. We chose to administer the dopamine precursor L-DOPA as a functional agonist and the selective D2/D3-antagonist amisulpride. L-DOPA is a natural DA-precursor and its potency is demonstrated by the fact that it is still the best Parkinson's drug (Muthuraman et al., 2018), while the D2/D3 receptor antagonist, amisulpride, has been reported to display selectivity for the limbic system in humans (Schoemaker et al., 1997). These compounds, as well as placebo, were applied in a randomized double-

blind within-subject design due to the superior power of cross-over designs (Wellek & Blettner, 2012); especially in pharmaco-fMRI.

Recent studies with DA drugs in healthy individuals have shown that different areas of the DA system react different to a DA challenge (Cole, Beckmann, Oei, Both, & Van Gerven, 2013; Martins, Mehta, & Prata, 2017). In particular, amisulpride decreased the striatum's response in a cue task (Hermann et al., 2006) and shifted the balance of orbitofrontal connectivity from associative areas towards the frontal cortex (Kahnt, Weber, Haker, Robbins, & Tobler, 2015). These results point to strategic neuroanatomical hubs like the striatum or the orbitofrontal cortex but lack the description of unifying mechanisms. In addition, many of the previous studies are limited to these (neurobiologically plausible) target regions and ignore the DA nuclei of the brain stem, most likely because they are difficult to depict in anatomical images and there have been no standardized masks from neuroanatomical atlases.

In ADHD, it is particularly important to understand the neural basis of impulsive behavior (Karam et al., 2017). It can be assumed that more impulsive people show a different pattern of neuronal response to DA stimulation, as previous studies have found evidence for altered dopamine receptor availability (Buckholtz et al., 2010), different response of the reward system (Hermann et al., 2006), and different connectivity of striatal nuclei depending on an individual's impulsivity during DA stimulation (Cole, Oei, et al., 2013).

Our main objectives were threefold. First, we were interested in whether there is an effect of DA midbrain nuclei on whole brain connectivity in response to a powerful pharmaco-challenge. Second, we wanted to test whether its direction is different for amisulpride and L-DOPA or whether L-DOPA and amisulpride show the same directionality in comparison to placebo. Specifically, we expected L-DOPA to have greater FC than amisulpride with region of interest (ROI) seed of the basal ganglia to the motor system and a same-direction relation for both drugs between striatal ROI seeds to the dorsal anterior cingulate as found by Cole, Beckmann, et al. (2013). And third, we wanted to investigate the relationship between FC of DA brain stem nuclei and impulsivity, as this enables a connection to psychiatric disorders with increased impulsivity (Dalley & Robbins, 2017; Nigg, 2017).

2 | METHODS

2.1 | Inclusion and exclusion criteria

Healthy volunteers of both sexes with an age between 18 and 50 years were included in this study. Participants were excluded in case of any serious, acute or chronic physical diseases, any history of psychiatric disorders or previous allergic drug response. Taking medication other than thyroid hormone replacement therapy or hormonal contraceptives was an exclusion criterion, as was pregnancy. Furthermore, for safety reasons, the volunteers were not allowed to show any contraindication to magnetic resonance imaging such as metallic objects in the body, tattoos with metal-containing ink, pacemakers, cochlear implants, claustrophobia, etc.

2.2 | Participants

Participants were recruited via local advertising measures. A total of 45 healthy volunteers (average age: 22.81 years, SD: 2.71 years) were included, of whom 23 were females. The average body weight of the subjects included was 72.86 kg (SD: 12.91 kg) with an average height of 1.75 m (SD: 0.11 m), which corresponds to an average BMI of 23.59 (SD: 3.08). The eligibility of the study participants regarding the inclusion and exclusion criteria was assessed in a medical consultation. The participants received an expense allowance of approx. 90 € for participation in the study.

The approval to conduct the study was given by the local ethics commission (Faculty of Medicine, University Hospital, Goethe University, Frankfurt am Main) and is subject to the Declaration of Helsinki of the "World Medical Association: Ethical Principles for Medical Research Involving Human Subjects" and the "Guidelines for Good Clinical Practices (GCP)". In addition, the study was registered as a clinical trial in the German study registry under the ID: DRKS00011209. Written informed consent was obtained from each volunteer before the start of the study.

2.3 | Behavioral measures

Participants filled out the German version of the UPPS Impulsive Behavior Scale (Schmidt, Gay, D'Acremont, & Van Der Linden, 2008; Whiteside & Lynam, 2003). The items were scored according to severity between 0 and 3 and a sum score was calculated based on the German version. Seven participants did not provide full information of the scale and were excluded from the correlation analysis with FC variables described below. The correlation analysis included $n = 38$.

2.4 | Experimental procedure: Drug application

The measurements were performed as a placebo-controlled, double-blind, three-stage cross-over study. In total, the volunteers were scheduled for three consecutive appointments at intervals of at least 4 days. The minimum interval between the fMRI measurements was chosen to ensure that at the time of the measurement, drugs from a previous measurement were eliminated from the body of the participants. The plasma half-life ($t_{1/2}$) of the pharmaceuticals used was considered, which is $t_{1/2} = 1\text{--}1.5$ h for L-3,4-Dihydroxyphenylalanin and $t_{1/2} = 17$ h for amisulpride. After five half-lives, it can be assumed that a drug has been sufficiently eliminated from the body and therefore cannot influence subsequent measurement.

The study participants received the study medication orally approximately 75 min before the start of the resting state measurement. At each session the subjects received either placebo, 125 mg levodopa, or 200 mg amisulpride. Each study participant hence received each of the medications exactly once in randomized order.

The placebo tablet used consisted of lactose powder packaged in gelatine capsules. The same gelatine capsules were used to package

the other pharmaceuticals to ensure blinding on both sides. The L-DOPA tablet used was a composition of 100 mg levodopa and 25 mg carbidopa, an aromatic L-amino acid decarboxylase that catalyzes the conversion of L-DOPA to dopamine. In contrast to levodopa, carbidopa does not cross the blood-brain barrier and thus only acts on the periphery of the body. Thus, the central availability of L-DOPA can be increased, since otherwise 95% of the levodopa would be decarboxylated in the periphery and would not be effective in the CNS (Muthuraman et al., 2018).

The unblinding did not take place until the MRI analysis of all volunteers had been completed. Both before and after each measurement, pulse per minute and blood pressure was measured in each subject. About 75 min after taking the drug, the fMRI resting-state fMRI measurement began. The waiting time between taking the medication and starting the resting-state fMRI measurement is based on the time (t_{\max}) until the maximum plasma concentration (C_{\max}) is reached. This is indicated with $t_{\max} = 0.5\text{--}1$ h, for L-DOPA (Contin & Martinelli, 2010) and with amisulpride a first plasma concentration peak is also observed 1 h after oral intake (Rosenzweig et al., 2002). During the 8-min resting-state measurements, the study participants were instructed to keep their eyes closed and to relax without falling asleep. In addition, the participants were encouraged to move as little as possible to prevent artifacts. After each measurement there was a 60-min follow-up period to rule out side-effects of the drugs.

2.5 | MRI measurement

The data acquisition was done with a 3 Tesla full body MR scanner (Siemens Magnetom Trio syngo MR A35, Brain Imaging Center, Frankfurt am Main) and an eight-channel head coil. As an anatomical sequence, a T1-weighted sequence (MPRAGE, magnetization prepared rapid acquisition gradient echo sequence) was measured and afterwards a gradient echo EPI sequence for the functional imaging data was performed. The sequence information for the MPRAGE sequence was as follows: repetition time (TR) = 1900 ms, echo time (TE) = 3.04 ms, TI = 900 ms, flip angle = 9°, FoV (field of view) = 256×256 mm, voxel size = $1 \times 1 \times 1$ mm. And for the EPI sequence: repetition time (TR) = 1800 ms, echo time (TE) = 30 ms, flip angle = 90°, FoV (field of view) = 192×192 mm, m, 28 layers with 4 mm, voxel size = $3 \times 3 \times 4$ mm. Details are described in Deichmann, Gottfried, Hutton, and Turner (2003). Foam pads were used to minimize head movements of participants.

2.6 | Movement artifacts

Movement can be the cause of artifactual connectivity patterns. To evaluate this, we calculated movement for each of the drug conditions based on the method proposed in Power, Barnes, Snyder, Schlaggar, and Petersen (2012). We calculated framewise displacement (FD) based on the rigid-body-model parameters from SPM12's realignment with $FD_i = |\Delta d_{ix}| + |\Delta d_{iy}| + |\Delta d_{iz}| + |\Delta \alpha_i| + |\Delta \beta_i| + |\Delta \gamma_i|$,

where $|\Delta d_{ix}| = d_{(i-1)x} - d_{ix}$. The variables x , y , and z refer to movement along the three axis in mm, the variables α , β , and γ refer to the rotation along these three axes. Rotational displacements were converted from degrees to millimeters by calculating displacement on the surface of a sphere of radius 50 mm, which is approximately the mean distance from the cerebral cortex to the center of the head.

2.7 | Data analysis: fMRI preprocessing

Images from $n = 45$ participants were realigned, slice-time corrected, spatially normalized to standard stereotaxic space (Montreal Neurological Institute [MNI] template), resampled to 3 mm isotropic voxels, and smoothed with 8 mm full-width at half maximum Gaussian kernel by using SPM12 (Flandin & Friston, 2008) in combination with the CONN-toolbox V1.8 for preprocessing (Whitfield-Gabrieli, 2012). A band-pass filter (0.01–0.1 Hz) was used to get rid of non-neural signals. Further noise correction was done by regressing out motion parameters derived from the realignment procedure and the first order derivative of movement parameters. Signal from the cerebrospinal-fluid and white-matter was regressed out with an aCompCor-strategy. This method (Behzadi, Restom, Liu, & Liu, 2007) takes the principal components of white matter/cerebrospinal fluid regions as regressors as nuisance regressors and is able to avoid the global-scaling related anticorrelation issues (Chai, Castañón, & Ongür, 2012).

We focused our seed-based FC analysis on regions that are central to the meso-limbic system, have a known link to the reward system and were reliably defined in the recently published OTI Atlas (Pauli, Nili, & Tyszka, 2018). This atlas was constructed based on high-spatial resolution T1- and T2-weighted structural images from 168 young adults. Tissue boundaries were used to delineate subcortical nuclei which were combined to form a probabilistic atlas. Out of the atlas' parcellated regions, we choose seven nuclei because of their link to reward and the DA system: putamen (Pu), accumbens (NAc), and caudate (Ca) as striatum (Pauli, O'Reilly, Yarkoni, & Wager, 2016) representing value and action selection, substantia nigra (SNr: rostral, SNc: caudal) and ventral tegmental area (VTA) as the basic midbrain sources of dopamine (Haber, Kim, Mailly, & Calzavara, 2006; Haber & Knutson, 2010) and the extended amygdala (EXA), a major limbic hub of the fear reaction system that is known to be strongly modulated by DA inputs (De Bundel et al., 2016).

2.8 | Data analysis: Group statistics

First-level correlation maps were calculated by extracting the residual BOLD-time course from the ROI seeds and correlating these with the other voxels within the brain. These correlation coefficient maps were then converted into a normally distributed z score (Fisher transformation). Transformed correlation maps were used for two-sided paired t tests on the second-level stage. As we had specific hypotheses, we report the direct comparisons L-DOPA versus placebo and amisulpride

versus placebo. To test a linear drug effect, we test L-DOPA > placebo > amisulpride (and the other direction), which equals a paired t test in a within subject design. To test a same-direction effect of both drugs, we tested the contrast amisulpride+L-DOPA > placebo (and the other direction), which equals a curvilinear or U-shaped effect in a within-subject design (compare Kessler, Angstadt, & Sripada, 2017) and amisulpride versus L-DOPA. For the between UPPS impulsivity (as a regression model), we focused on the influence of L-DOPA on VTA connectivity because of VTA's link to motivational behavior in a subsample of $n = 38$. For the within-subject condition we used the L-DOPA versus placebo contrast, and for the between-subject contrast, we included the UPPS score as a covariate. The correlation with UPPS was performed using the same FC methodology with the only difference that UPPS was included as a covariate in the paired t test L-DOPA versus placebo. For correction of multiple testing during second-level statistics we used cluster-wise whole-brain analysis with topological FDR correction $pFDR < 0.05$ (cluster defining voxel threshold $p < .001$) (Chumbley, Worsley, Flandin, & Friston, 2010). While more liberal thresholds are prone to false-positives, recent methodologic studies established this as a conservative threshold (Kessler et al., 2017). For post hoc analysis of interaction with the default-mode network (DMN), we used a region-of-interest mask for small volume correction. The DMN mask was defined according to prior research (Shirer, Ryali, Rykhlevskaia, Menon, & Greicius, 2012) from a 90-component parcellation and includes the dorsal DMN, ventral DMN, and precuneus networks (images accessible via https://neurovault.org/media/images/955/DMN_151021_pycortex/index.html).

3 | RESULTS

3.1 | Connectivity main effects

To validate our seed-based connectivity approach and to enable comparison with alternative seed-based ROIs, we calculated seed-maps of the placebo condition to illustrate the connectivity's main effect. Putamen and caudate show connectivity with other parts of the basal ganglia, the anterior cingulate gyrus, the medial orbitofrontal gyrus and the insula among others. The mesencephalic nuclei (SNc/r, VTA) show a strong connectivity to the striatum, the rostral SNr to the medial orbitofrontal cortex. The extended amygdala and the nucleus accumbens are connected to the medial temporal lobe, especially the hippocampus, the insula and the orbitofrontal gyrus. A detailed overview is given in the Figure S1.

3.2 | Influence of drugs on movement

The mean values of the change of movement were obtained under placebo as well as L-DOPA and amisulpride: L-DOPA mean FD 0.19 standard deviation 0.08, placebo mean FD 0.19 standard deviation 0.08 and amisulpride mean FD 0.18 standard deviation 0.06. According to the Kolmogorov–Smirnov-test, values were not normally distributed. For this reason, we used the Wilcoxon-sign-test. None of the comparisons between drug-sessions gave significant differences:

L-DOPA versus placebo $p = .88$, amisulpride versus placebo $p = .51$ and L-DOPA versus placebo $p = .41$.

3.3 | Connectivity changes during L-DOPA

When comparing connectivity changes after L-DOPA administration in comparison to placebo, we noticed mainly an increase in FC from the seeds caudate, substantia nigra and VTA (Table 1). The caudate more strongly connected with a cluster of the central operculum, the substantia nigra (both rostral and caudal) more strongly linked to bilateral cluster spanning the insula and the operculum (Table 1). The lowest p value were found for the ROI seeds VTA and the SNc with an increase in connectivity to the left insula (see Figure 1a and Table 1).

There was a decrease in connectivity during the L-DOPA condition in the seed regions caudate, nucleus accumbens, and extended amygdala. All seeds showed a decrease to clusters comprising mainly the medial prefrontal cortex, with the seed caudate showing the most significant effect and the biggest cluster (Table 1).

To validate whether this cluster belongs to the DMN, we used a ROI mask of the DMN for post hoc analysis. The EXA-seed led to a

significant cluster in this dorsal DMN ROI (cluster corrected $pFDR = 0.005$, $k = 114$, $MNI = -2/50/-18$), the caudate-seed led to a significant cluster in the dorsal DMN ROI (cluster corrected $pFDR < 0.001$, $k = 346$, $MNI = -8/54/0$), the NAc-seed showed only a trendwise effect (cluster corrected $pFDR = 0.057$, $k = 67$, $MNI = -2/50/-18$).

3.4 | Connectivity changes during amisulpride

The DA antagonism induced by the amisulpride challenge led to an increase in connectivity from the ROI seed putamen as well as from the ROI seed nucleus accumbens (Table 2). The putamen's connectivity to the precuneus was increased (see Figure 1b and Table 2) as well as the connectivity between the nucleus accumbens and the supplemental motor cortex.

Amisulpride decreased seed connectivity from the rostral substantia nigra to the postcentral gyrus and the cerebellum (Table 2).

We performed a post hoc analysis with a DMN ROI mask for verifying whether the precuneus cluster during putamen FC amisulpride > placebo is part of the DMN. However, this was not significant. On visual inspection, this precuneus cluster lay dorsal of the typical DMN (see Figure 1b and Table 2).

TABLE 1 Positive correlations of functional connectivity of seed regions from the "probabilistic in vivo atlas" of Pauli et al. under levodopa, compared with placebo (L-DOPA > placebo and placebo > L-DOPA)

Seed region	Brain region	Cluster size	MNI-coordinates			pFDR
			x	y	z	
L-DOPA > placebo						
Ca	Gyrus precentralis L, central operculum L	219	60	+2	+4	0.003
SNc	Central operculum L, gyrus precentralis L	746	-50	-14	+10	0.003
	Central operculum R	305	60	-20	+30	0.0004
	Polus temporalis R	150	34	+4	-48	0.019
	Centrale operculum R, insula R	138	48	-2	+12	0.02
	Insula L, central operculum L	113	-34	+0	+12	0.037
	Insula R, frontal operculum R	102	40	+16	-2	0.045
SNr	Precentral gyrus L	339	-46	-6	+28	0.0005
	Gyrus supramarginalis L	251	-56	-52	+36	0.002
	Insula R	225	44	+12	-4	0.002
	Polus temporalis L	197	-56	+12	-6	0.004
	Insula L, central operculum L	156	-34	+0	+12	0.012
	Lateral occipital cortex L	146	-12	-78	+52	0.014
	Central operculum R, parietal operculum R	126	58	-18	+20	0.023
VTA	Central operculum L, insula L	548	-32	+2	+12	0.000002
Placebo > L-DOPA						
Ca	Paracingulate gyrus (L/R), R medial prefrontale cortex	439	-8	+54	+0	0.000009
NAC	Medial prefrontale cortex	113	-2	+50	-18	0.046
EXA	Medial prefrontale cortex	138	-2	+50	-18	0.018

Note: The table shows significant cluster, their size in voxel, and their localization in the MNI space as MNI coordination in the order x y z. The threshold for cluster correction was set at $p < .001$. Only significant seed regions are shown.

Abbreviations: Pu, putamen; CA, nucleus caudatus; NAC, nucleus accumbens; EXA, extended Amygdala; SNc, substantia nigra pars compacta; SNr, substantia nigra pars reticularis; VTA, area tegmentalis ventralis; L, left; R, right.

FIGURE 1 (a–c) Connectivity changes from selected seed ROIs during different drug conditions. The left column shows in A, B, and C the seed region masks from the substantia nigra (SNc), the putamen (Pu) and the extended amygdala (EXA). The axial and sagittal slices show the most significant cluster for the specified and its location. The color coding bar depicts the voxel-wise T values. The column with bar plots on the right shows the mean beta values extracted from the respective cluster for all drug conditions. Conditions that were not explicitly included in the contrast are filled with lighter blue and are shown to illustrate linear effects. The specific contrast image on the left is linked via a blue arrow to its corresponding barplots on the right

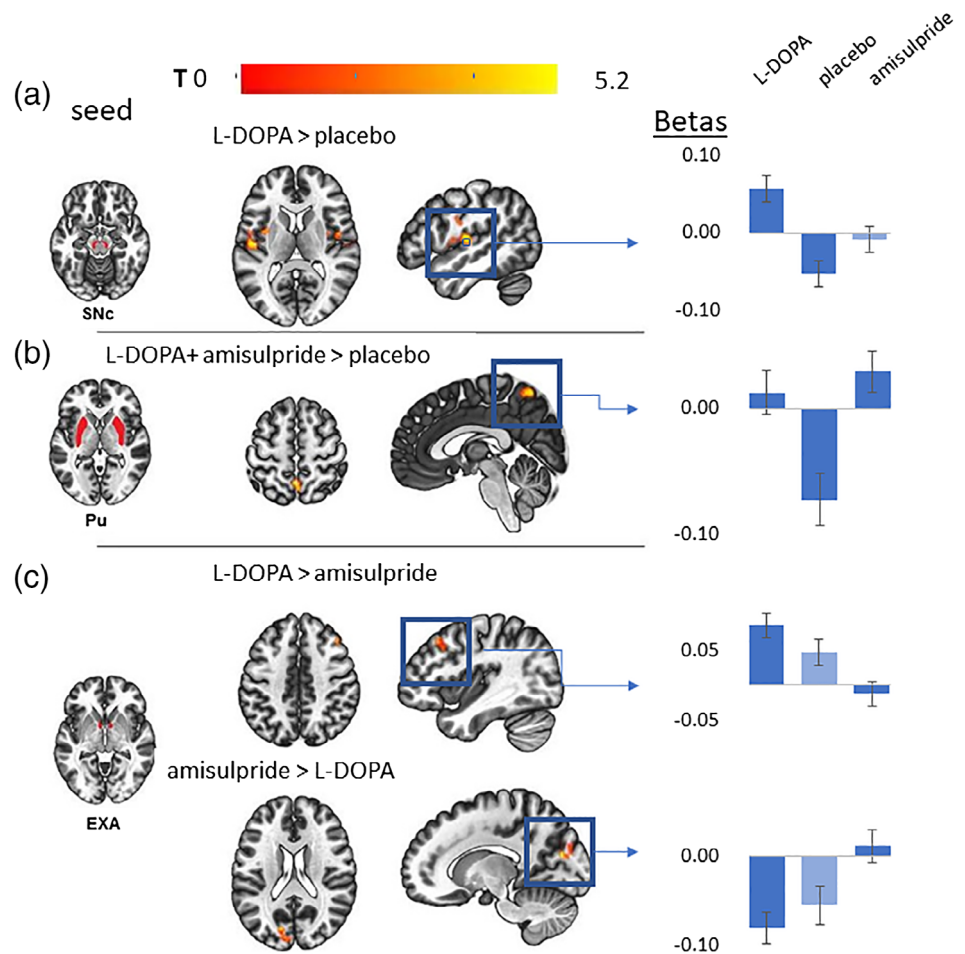


TABLE 2 Positive correlations of functional connectivity of seed regions from the “probabilistic in vivo atlas” of Pauli et al. under amisulpride compared with placebo (amisulpride vs. placebo)

Seed region	Brain region	Cluster size	MNI-coordinates			pFDR
			x	y	z	
Amisulpride > placebo						
Pu	Precuneus	186	-2	-54	+58	0.001
NAC	Supplemental motor cortex (L + R)	146	-2	-28	+54	0.008
	Precentral gyrus (L + R)					
Placebo > Amisulpride						
SNr	Postcentral gyrus (L)	112	-44	-32	+58	0.021
	Cerebellum (L)	110	-44	-76	-46	0.021

Note: The table shows significant cluster, their size in voxel, and their localization in the MNI space as MNI coordination in the order x y z . The threshold for clusters was set at $p < .001$. Only significant seed regions are shown.

Abbreviations: Pu, putamen; CA, nucleus caudatus; NAC, nucleus accumbens; EXA, extended Amygdala; SNc, substantia nigra pars compacta; SNr, substantia nigra pars reticularis; VTA, area tegmentalis ventralis; L, left; R, right.

3.5 | Differential connectivity changes between amisulpride and L-DOPA

There was an increase from putamen to the fusiform gyrus, from the accumbens to the temporal lobe and from the extended amygdala to

the prefrontal cortex (Figure 1c and Table 3). Both rostral and caudal substantia nigra increased their FC to the cerebellum.

The connectivity between the extended amygdala and the precuneus increased for the comparison amisulpride > L-DOPA (see Figure 1c and Table 3).

TABLE 3 Positive correlations of functional connectivity of seed regions from the “probabilistic in vivo atlas” of Pauli et al. under levodopa, compared with amisulpride (amisulpride vs. L-DOPA)

Seed region	Brain region	Cluster size	MNI-coordinates			pFDR
			x	y	z	
L-DOPA > Amisulpride						
Pu	Gyrus Fusiformis R, hippocampus R, gyrus parahippocampalis R	205	32	-20	-24	0.005
NAC	Gyrus temporalis inferior L, lateral occipital cortex L	228	-58	-64	-12	0.002
EXA	Gyrus frontalis medius R	126	40	+26	+44	0.04
SNC	Cerebellum R	366	18	-48	-50	0.0002
SNr	Gyrus supramarginalis R,	644	64	-34	+44	0.000001
	Cerebellum R	522	12	-46	-62	0.000004
	Gyrus supramarginalis L, gyrus postcentralis L	364	-48	-40	+50	0.00008
	Cerebellum L	286	-20	-66	-58	0.0004
	Lateral occipital cortex L	195	-22	-72	+38	0.003
Amisulpride > L-DOPA						
EXA	Cuneus L, Polus occipitalis L	334	-14	-78	+20	0.00007

Note: The table shows significant cluster, their size in voxel, and their localization in the MNI space as MNI coordination in the order x y z. The threshold for clusters was set at $p < .001$. Only significant seed regions are shown.

Abbreviations: Pu, putamen; CA, nucleus caudatus; NAC, nucleus accumbens; EXA, extended amygdala; SNC, substantia nigra pars compacta; SNr, substantia nigra pars reticularis; VTA, area tegmentalis ventralis; L, left; R, right.

Seed region	Brain region	Cluster size	MNI-coordinates			pFDR
			x	y	z	
L-DOPA + Amisulpride > placebo						
Pu	Precuneus	214	-02	-52	+60	0.001
EXA	R inferior frontal gyrus	136	+02	+12	+20	0.02
SNC	Insula L, central operculum R	154	-56	-14	+8	0.02
	Insula R, central operculum L	104	+46	-08	+08	0.04

Note: The table shows significant cluster, their size in voxel, and their localization in the MNI space as MNI coordination in the order x y z. The threshold for clusters was set at $p < .001$. Only significant seed regions are shown.

Abbreviations: Pu, putamen; CA, nucleus caudatus; NAC, nucleus accumbens; EXA, extended Amygdala; SNC, substantia nigra pars compacta; SNr, substantia nigra pars reticularis; VTA, area tegmentalis ventralis; L, left; R, right.

3.6 | Differential connectivity changes between amisulpride and L-DOPA versus placebo

These results correspond to a U-shaped or curvilinear DA relation in a within-subject design. We observed an increase of FC from the putamen to the precuneus (Figure 1b), from the caudal substantia nigra to the bilateral operculum/insula and from the extended amygdala to the right inferior frontal gyrus (Table 4).

3.7 | Correlation of impulsivity with FC after DA stimulation

We ran a voxel-wise correlation between the between-subject factor UPPS score and the within-subject factor L-DOPA versus placebo. We

TABLE 4 Positive correlations of functional connectivity of seed regions from the “probabilistic in vivo atlas” of Pauli et al. under levodopa and amisulpride compared with placebo (L-DOPA + amisulpride vs. L-DOPA)

considered this the most interesting contrast because of its statistical significance and its plausible link to neurobiology. To avoid a circular “voodoo correlation” (Kriegeskorte, Simmons, Bellgowan, & Baker, 2009; Vul & Pashler, 2017) we did not simply extract the FC from our significant cluster in the right striatum but choose a voxelwise cluster-corrected comparison with VTA as seed region.

We did not observe significant correlations with the previously reported regions in the striatum, but found a cluster on the border of the anterior to the posterior gyrus cinguli which, during L-DOPA challenge, showed a strong linear positive correlation between UPPS impulsivity (MNI coordinates +06, -16, -36, cluster size $k = 141$, $pFDR = 0.035$, $r = 0.71$, $p < .001$ uncorrected for maximum cluster), see Figure 2. There was no significant correlation with UPPS during the placebo condition only ($pFDR > 0.75$) or during the placebo versus amisulpride condition ($pFDR > 0.67$).

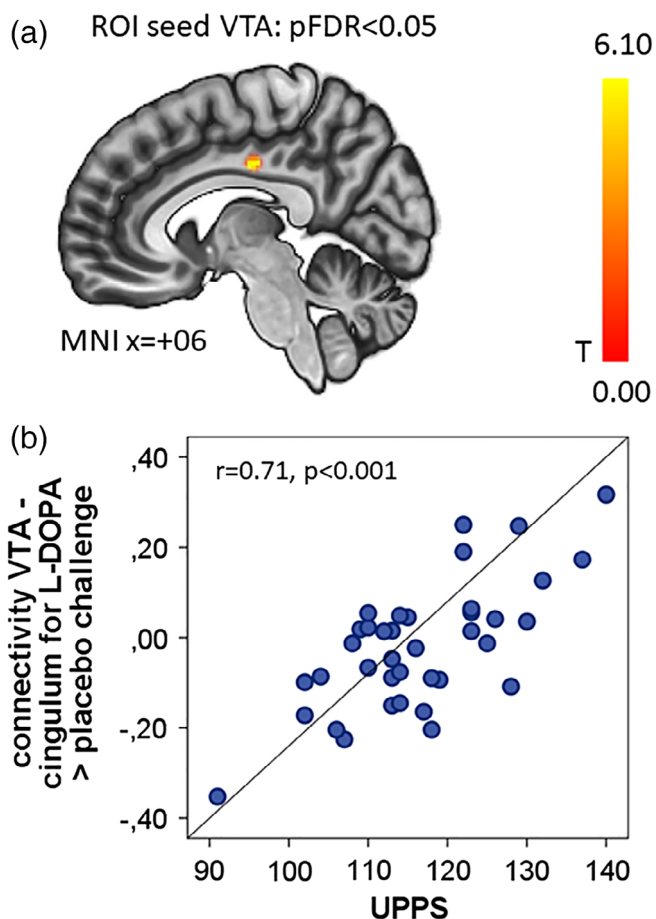


FIGURE 2 Impulsivity modulates VTA-mid-cingulum connectivity for L-DOPA > placebo. (a) Sagittal view of the significant cluster (MNI coordinates +06, -16, -36) correlated with UPSS impulsivity sum score from the seed VTA for L-DOPA > placebo. Color bar gives T values. (b) Scatterplot with the extracted mean correlation from the cluster specified above and UPSS impulsivity. The correlation coefficient r is shown with an uncorrected p value calculated from the mean extracted beta value

4 | DISCUSSION

Our study probed the functional architecture and neuroanatomy of the DA system, which led to two main findings. Our first main findings are the differential modulation of FC during L-DOPA and amisulpride administration for specific subcortical seed regions. Our second main finding shows that the L-DOPA-challenge leads to different FC changes between VTA and cingulate gyrus in more impulsive participants.

L-DOPA had the most significant effects versus placebo for the ROI seed VTA and the SN. L-DOPA significantly increased the connectivity between these midbrain DA nuclei and a large cluster comprising the central operculum, the left insula, postcentral gyrus, and left putamen. The insula and operculum form an important hub of the mesolimbic reward system, which is mainly known for its role in reward anticipation. While the effect was stronger for L-DOPA, than for amisulpride, both contributed to an increase of connectivity, pointing to a possible curvilinear effect of SNc-FC to the operculum/

insula. Apart from its well-known role in reward (Liu, Hairston, Schrier, & Fan, 2011), the operculum plays a role in food reward expectation (Stice, Yokum, Bohon, Marti, & Smolen, 2010) and integrates exteroceptive–interoceptive signals (especially when lying in the scanner) that are necessary for interoceptive awareness (Blefari et al., 2017). The increased coupling of DA mesencephalic nuclei and the insula and operculum points to a L-DOPA mediated switch to interoceptive processing.

This strong L-DOPA-dependent effect of mesencephalic seed regions indicates that the DA nuclei are the prime source of modulatory changes for L-DOPA, consistent with the mechanism of action of L-DOPA as a DA precursor, which is converted rapidly in soma of mid-brain DA neurons (Westerink & Korf, 1976). Enhancing DA formation in these cells might then augment DA neurotransmission to target regions, such as those indicated by our data. Characterization of DA modulation in resting-state networks has been tried in previous studies with different results (Cole, Beckmann, et al., 2013; Flodin, Gospic, Petrovic, & Fransson, 2012; Kelly et al., 2009).

In a double-blind, parallel group design using placebo, L-DOPA and haloperidol, Cole et al. found a linear decrease from the basal ganglia FC to the motor cortex in the contrast L-DOPA < placebo < amisulpride. While this is similar to our L-DOPA > amisulpride FC effect, this study did not report a curvilinear effect of L-DOPA + amisulpride > placebo for an increase of SNc FC to the bilateral operculum. Strong methodological differences make direct comparison between the studies difficult. We used a ROI seed approach, whereas (Cole, Beckmann, et al., 2013) used a group-ICA approach, a more liberal statistical threshold, a less powerful parallel-groups-design and only male participants. As women show higher L-DOPA bioavailability (Kompolti et al., 2002), this might point to a higher L-DOPA sensitivity in our study. Kelly et al. found in a smaller study ($n = 19$) an increase in FC between putamen, brainstem and cerebellum and L-DOPA increased FC between the ventral striatum and the prefrontal cortex, while decreasing FC between ventral striatal and the DMN (Kelly et al., 2009). Flodin et al. report, in a small pharmacofMRI study that L-DOPA mainly decreased connectivity from the ROI seed amygdala to inferior frontal gyri and midline regions of the DMN (Flodin et al., 2012). While the linear increase of FC from ROI seed SNc to areas of the motor system (in our case mostly cerebellum) during L-DOPA > amisulpride parallels findings of more FC between basal ganglia and motor cortex in Cole, Beckmann, et al. (2013), the increase of connectivity between DA midbrain nuclei and the operculum/insula during L-DOPA has not been reported before. Interestingly, the ROI seed SNc shows a higher FC for both amisulpride and L-DOPA to the bilateral operculum, pointing to a possible curvilinear effect. However, L-DOPA seems to be the main driver of the effect as its increase in FC to the operculum/insula generalizes to other midbrain nuclei (VTA/SNr) and has higher effect sizes.

This spatial specificity of the L-DOPA-induced FC increase from DA brain stem nuclei to cortical and subcortical regions has not yet been reported in human pharmacofMRI studies. The most likely explanation is that we used a specifically designed VTA/SN-mask that was not previously available; additionally, the power of our study was

much higher due to our relatively large sample through the use of a cross-over design (Hills & Armitage, 1979) in comparison to simpler parallel-group designs.

In contrast to the strong effect of L-DOPA on midbrain nuclei seeds, we expected an antagonistic effect of the postsynaptic D2/D3 receptor antagonist amisulpride (Rosenzweig et al., 2002). In addition, in doses lower than 100 mg it may increase DA transmission via presynaptic autoreceptors, an effect which has found clinical use in the treatment of depression. Therefore, at lower doses, amisulpride might facilitate DA transmission via presynaptic autoreceptors, whereas at higher doses (>50 mg), the dopamine-antagonistic effects will dominate. In a previous rs-fMRI study in $n = 19$ volunteers (Metzger, Wieggers, Walter, Abler, & Graf, 2015), the authors reported a modulation of local rs-activity of regions in the putamen correlating with amisulpride plasma levels and an increase of rs-FC between regions of the DA pathway comprising the SN and putamen. This was interpreted as a possible pro-DA effect in lower dose (200 mg). However, human SPECT binding suggest a predominant antagonistic effect via a D2 receptor occupancy between 60 and 80% for 200 mg amisulpride (la Fougère et al., 2005). In our larger sample using advanced methodology, we were not able to find an increase between putamen and VTA/SN FC following the 200 mg amisulpride challenge in contrast to large increase after L-DOPA administration; arguing against a pro-DA effect on a large-scale systems level. Amisulpride decreased connectivity between SNr and the cerebellum, which is consistent with the role of the D3-receptor in the cerebellum (Barik & de Beaufort, 1996). During DA-blockade with amisulpride, as well as during the contrast amisulpride and L-DOPA versus (see Figure 1b and Table 4), the connectivity between the putamen and the precuneus increased significantly, suggesting a curvilinear effect of dopamine on the putamen-precuneus connectivity. While the precuneus is a central hub of the DMN (Cunningham, Tomasi, & Volkow, 2017), the cluster of our study was located above a standard DMN-mask and was not significant in this DMN-ROI. Nevertheless, a recent study independently shows the influence of DA modulation of FC between striatum-precuneus (Birn et al., 2019). The functional role of the balance between striatum and precuneus FC during DA modulation remains unclear and more studies are warranted.

There was an effect of DA tone on different spatial aspects of a network of the dorsolateral prefrontal cortex (DLPFC, Brodmann area 9), the amygdala and the visual cortex. The DLPFC is a strong modulator and inhibitor of the amygdala (Urry et al., 2006) and the amygdala is an important driver of occipital cortical activity (Amaral, Behnia, & Kelly, 2003; Vuilleumier, Richardson, Armony, Driver, & Dolan, 2004). In our study, the L-DOPA DA-boost increased the BA9-EXA FC in comparison to the dopamine blockade by amisulpride, whereas amisulpride DA-blockade increased the limbic-visual cortex connectivity in comparison to L-DOPA. The extended amygdala is a major hub for the evaluation of aversive stimuli connected to fear and anxiety (Davis, Walker, Miles, & Grillon, 2010). Its link to the DA system is via an efferent DA pathway originating in the VTA (Fudge & Emiliano, 2003). While the detailed feedback-circuit of VTA-EXA, and vice versa, cannot be derived from rs-fMRI, our experiment is the first in

humans showing complementary effect of L-DOPA and amisulpride on top-down and bottom-up connectivity of the EXA-network. L-DOPA (in comparison with placebo) induced a lower connectivity to parts of the medial PFC and precingulate cortex belonging to the DMN with the caudate and extended amygdala. This suggests a decoupling of certain reward-related brain areas with the DMN as a function of dopamine.

Contrary to our expectations, we did not observe an effect in the same direction from both drugs and FC between the basal ganglia and the mid-cingulate cortex as reported by Cole, Beckmann, et al. (2013). Interestingly, this specific region was found in a correlation analysis between DA modulation and impulsivity and is discussed below in detail.

In summary, our result might fit best into a model where the salience network, driven by mesencephalic DA nuclei, switches between executive networks and the DMN as described in previous studies showing a general effect of dopamine on task-based networks (Boehler et al., 2011). This salience network is composed of the anterior insula, the dorsal anterior cingulate cortex, VTA, ventral striatum, thalamus and amygdala. It is mainly found when important, "salient" stimuli in complex functions like communication, social behavior or self-awareness are processed and filtered (Menon, 2015).

In line with previous pharmaco-fMRI findings (Cole, Beckmann, et al., 2013), the effect of a DA modulation on ROI-seed coupling might reflect how brain DA acts on the dynamic balance between processes of flexible updating and cognitive stabilization (Cools & D'Esposito, 2011). Thus, our finding of decreased caudate-mPFC coupling during L-DOPA-mediated dopamine-boost reflects this role of the DA-system in network switching between salience and DMN networks (Boehler et al., 2011). This could be a marker for efficient cognitive functioning, which is disturbed in DA disorders like Parkinson's disease, schizophrenia or ADHD. As these switches might happen on a rapid time frame, future analysis should incorporate so-called sliding window approaches to study DMN-salience network coupling (Allen et al., 2014; Fong et al., 2019).

Our second main finding is that individual impulsivity on a behavioral level is correlated with VTA-cingulum connectivity during the increase of dopamine (the L-DOPA vs. placebo contrast). Such effects of DA subcortical nuclei on impulsivity have been described before in rodents during different decision paradigms (Dalley et al., 2007). Previous research demonstrated an effect of the dopamine-agonist bromocriptine in a working memory task on frontostriatal activity (Cools, Sheridan, Jacobs, & D'Esposito, 2007). This is in line with our observation of a link between dopamine, impulsivity and potential switching between salience- or task-related networks in contrast to DMN. While the cingulum's connectivity is not directly changed by the DA intervention in our task, its reactivity predicts individual impulsivity. Several other groups reported correlations between different measures of impulsivity and changes in DA networks (Cole, Oei, et al., 2013; Piray, den Ouden, van der Schaaf, Toni, & Cools, 2017), but none so far have observed an increase of VTA-cingulum FC during a DA boost. Our finding is located in the mid-cingulate cortex, a region known to have a rich DA innervation (Mark Williams & Goldman-

Rakic, 1998). While we cannot derive from our data whether this is a direct anatomical link or mediated via a second node (e.g., thalamus, see (Vogt, 2016)), the cingulum has important DA afferents and it has been implicated in reward assessment (for a thorough review on histochemistry and neuroanatomy cf Vogt, 2016) as well as psychiatric disorders like ADHD with impulsive behavior (Bush, 2011; Shin & Bush, 2011).

Our findings offer some interesting perspectives for ADHD or schizophrenia. In schizophrenic patients, VTA connectivity to the thalamus was increased as a result of 1-week antipsychotic treatment. Pre-treatment VTA connectivity with the default mode network was a predictor of low treatment response (Hadley et al., 2014). While our main effect shows a strong connectivity change from SN/VTA, we did not find a change of VTA-DMN connectivity during amisulpride challenges. The dysregulated, DA switching between reward-related FC and the DMN is not directly found in our sample, however the decrease of FC between caudate, EXA, accumbens, and the mPFC (as part of the DMN) during L-DOPA challenge points to the crucial role of dopamine in mediating FC between parts of the DMN and the reward-related salience network. The VTA/SN-connectivity to the DMN and limbic system has a characteristic developmental trajectory and showed a specific change in ADHD patients (Tomasi & Volkow, 2014). As we demonstrate the change of VTA/SN-connectivity to the Insula during L-DOPA, this indicates that VTA/SN-seed-based rsfMRI might capture certain features of the DA system. Judging from our study, the aforementioned neuroimaging findings in schizophrenia and ADHD seem to be the direct expression of a dysregulated DA system.

While our study has several strengths, such as large sample size (for a mono-centric pharmacofMRI study), good validity of neuroanatomical connectivity and two complementary drugs in relation to placebo, we nevertheless would like to point out some limitations. FC is purely correlational, its major and inherent limitation is that the directionality of the connectivity effects is hard to measure. While we describe connectivity patterns of the VTA and rostral and caudal SN, we are aware that rs-fMRI in our technical setting might not be optimal in delineating these neuroanatomical different nuclei reliably. Nevertheless, the main statement, that DA midbrain nuclei change their connectivity under a DA-boost still holds true even if we cannot precisely differentiate between VTA and SN. Furthermore, the changes in connectivity patterns are more complex than in our hypothesis. This is especially true for amisulpride, which is not a simple blocker of D2-related striatal connectivity and showed together with L-DOPA for example, a nonlinear response between SNc and putamen and between extended amygdala and IFG. While seed-to-voxel FC analysis seems to give good power for our crossover-within-subject design, future analysis should make use of methods which might give better insight into complex connectivity changes like graph theory analysis. The aforementioned interpretation of linear or curvilinear effects is somewhat speculative. For a thorough understanding of linear or curvilinear effects, one would need to titrate different drug doses, which is beyond the possibilities of a repeated-measure cross-over design.

Our results show different functional effects of dopamine neuromodulations at the system level between seed regions of subcortical nuclei. We show specific connectivity patterns for different subcortical nuclei that vary according to DA modulation and are related to impulsivity during a DA boost. These findings warrant further experiments using specific task-based, reward-related paradigms in healthy volunteers as well as patients suffering from a dysregulation of the DA system. As we demonstrate a strong effect of L-DOPA on the connectivity of DA midbrain nuclei and on changes in VTA-mid-cingulum connectivity depending on impulsivity, it would be interesting to investigate how the brain of patients with high impulsivity (e.g., ADHD, substance abuse, etc.) would behave under DA challenge and whether connectivity data under DA stimulation are complementary to DA binding studies, for example, C11-raclopride-PET for dopamine-receptor availability. In the future, a L-DOPA challenge might be used to specifically challenge midbrain-connectivity given sufficient sample size for a variety of translational questions. Additionally, pharmacofMRI of DA stimulation is unlikely to model all aspects of complex psychiatric conditions such as ADHD or schizophrenia, but components of such syndromes may be investigated using more sophisticated pharmacofMRI protocols.

ACKNOWLEDGMENTS

Financial support for this study was received from the European Union's Horizon 2020 research and innovation program under grant agreement 667302: Comorbid Conditions of ADHD (CoCA). Prof. Dr. Andreas Reif received personal fees from MEDICE Arzneimittel Pütter GmbH & Co. KG, Shire PLC, neuraxpharm Arzneimittel GmbH, Janssen-Cilag GmbH and Servier Deutschland GmbH present or during 36 months prior to publication. Oliver Grimm received personal fees from MEDICE Arzneimittel Pütter GmbH & Co. KG. No competing interests are disclaimed.

DATA AVAILABILITY STATEMENT

Data can be made available on reasonable request and fulfillment of ERB and German data protection law.

ORCID

Oliver Grimm  <https://orcid.org/0000-0002-0767-0301>

REFERENCES

- Allen, E. A., Damaraju, E., Plis, S. M., Erhardt, E. B., Eichele, T., & Calhoun, V. D. (2014). Tracking whole-brain connectivity dynamics in the resting state. *Cerebral Cortex*, 24(3), 663–676 Available from: <http://cercor.oxfordjournals.org/content/early/2012/11/09/cercor.bhs352.long>
- Amaral, D. G., Behnia, H., & Kelly, J. L. (2003). Topographic organization of projections from the amygdala to the visual cortex in the macaque monkey. *Neuroscience*, 118(4), 1099–1120 Available from: <http://www.ncbi.nlm.nih.gov/pubmed/12732254>
- Barik, S., & de Beurepaire, R. (1996). Evidence for a functional role of the dopamine D3 receptors in the cerebellum. *Brain Research*, 737(1–2), 347–350 Available from: <https://www.sciencedirect.com/science/article/pii/000689939600964X>

- Behzadi, Y., Restom, K., Liu, J., & Liu, T. T. (2007). A component based noise correction method (CompCor) for BOLD and perfusion based fMRI. *NeuroImage*, 37(1), 90–101 Available from: <http://www.pubmedcentral.nih.gov/articlerender.fcgi?artid=2214855&tool=pmcentrez&rendertype=abstract>
- Birn, R. M., Converse, A. K., Rajala, A. Z., Alexander, A. L., Block, W. F., McMillan, A. B., ... Populin, L. C. (2019). Changes in endogenous dopamine induced by methylphenidate predict functional connectivity in nonhuman primates. *The Journal of Neuroscience*, 39(8), 1436–1444 Available from: <http://www.ncbi.nlm.nih.gov/pubmed/30530859>
- Blefari, M. L., Martuzzi, R., Salomon, R., Bello-Ruiz, J., Herbelin, B., Serino, A., Blanke, O. (2017). Bilateral Rolandic operculum processing underlying heartbeat awareness reflects changes in bodily self-consciousness. *European Journal of Neuroscience*, 45(10), 1300–1312 Available from: <http://doi.wiley.com/10.1111/ejn.13567>
- Boehler, C. N., Hopf, J.-M., Krebs, R. M., Stoppel, C. M., Schoenfeld, M. A., Heinze, H.-J., Noesselt, T. (2011). Task-load-dependent activation of dopaminergic midbrain areas in the absence of reward. *The Journal of Neuroscience*, 31(13), 4955–4961 Available from: <http://www.jneurosci.org/content/31/13/4955.full>
- Buckholz, J. W., Treadway, M. T., Cowan, R. L., Woodward, N. D., Li, R., Ansari, M. S., ... Zald, D. H. (2010). Dopaminergic network differences in human impulsivity. *Science*, 329(5991), 532.
- Bush, G. (2011). Cingulate, frontal, and parietal cortical dysfunction in attention-deficit/hyperactivity disorder. *Biological Psychiatry*, 69(12), 1160–1167. <https://doi.org/10.1016/j.biopsych.2011.01.022>
- Chai, X. J., Castañón, A. N., Ongür, D., & Whitfield-Gabrieli, S. (2012). Anticorrelations in resting state networks without global signal regression. *NeuroImage*, 59(2), 1420–1428 Available from: <http://www.pubmedcentral.nih.gov/articlerender.fcgi?artid=3230748&tool=pmcentrez&rendertype=abstract>
- Chumbley, J., Worsley, K., Flandin, G., & Friston, K. (2010). Topological FDR for Neuroimaging. *NeuroImage*, 49(4), 3057–3064 Available from: <http://www.pubmedcentral.nih.gov/articlerender.fcgi?artid=3221040&tool=pmcentrez&rendertype=abstract>
- Cole, D. M., Beckmann, C. F., Oei, N. Y. L., Both, S., Van Gerven, J. M. A., & Rombouts, S. A. R. B. (2013). Differential and distributed effects of dopamine neuromodulations on resting-state network connectivity. *NeuroImage*, 78, 59–67.
- Cole, D. M., Oei, N. Y. L., Soeter, R. P., Both, S., Van Gerven, J. M. A., Rombouts, S. A. R. B. (2013). Dopamine-dependent architecture of cortico-subcortical network connectivity. *Cerebral Cortex*, 23(7), 1509–1516.
- Contin, M., & Martinelli, P. (2010). Pharmacokinetics of levodopa. *Journal of Neurology*, 257(S2), 253–261 Available from: <http://www.ncbi.nlm.nih.gov/pubmed/21080186>
- Cools, R., & D'Esposito, M. (2011). Inverted-U-shaped dopamine actions on human working memory and cognitive control. *Biological Psychiatry*, 69(12), e113–e125 Available from: <http://www.ncbi.nlm.nih.gov/pubmed/21531388>
- Cools, R., Sheridan, M., Jacobs, E., & D'Esposito, M. (2007). Impulsive personality predicts dopamine-dependent changes in Frontostriatal activity during component processes of working memory. *The Journal of Neuroscience*, 27(20), 5506–5514 Available from: <http://www.ncbi.nlm.nih.gov/pubmed/17507572>
- Cunningham, S. I., Tomasi, D., & Volkow, N. D. (2017). Structural and functional connectivity of the precuneus and thalamus to the default mode network. *Human Brain Mapping*, 38(2), 938–956 Available from: <http://doi.wiley.com/10.1002/hbm.23429>
- Dalley, J. W., Fryer, T. D., Brichard, L., Robinson, E. S. J., Theobald, D. E. H., Lääne, K., ... Robbins, T. W. (2007). Nucleus accumbens D2/3 receptors predict trait impulsivity and cocaine reinforcement. *Science*, 315(5816), 1267–1270.
- Dalley, J. W., & Robbins, T. W. (2017). Fractionating impulsivity: Neuropsychiatric implications. *Nature Reviews. Neuroscience*, 18(3), 158–171 Available from: <http://www.nature.com/articles/nrn.2017.8>
- Davis, M., Walker, D. L., Miles, L., & Grillon, C. (2010). Phasic vs sustained fear in rats and humans: Role of the extended amygdala in fear vs anxiety. *Neuropsychopharmacology*, 35, 105–135.
- De Bundel, D., Zussy, C., Espallergues, J., Gerfen, C. R., Girault, J. A., & Valjent, E. (2016). Dopamine D2 receptors gate generalization of conditioned threat responses through mTORC1 signaling in the extended amygdala. *Molecular Psychiatry*, 21(11), 1545–1553.
- Deichmann, R., Gottfried, J. A., Hutton, C., & Turner, R. (2003). Optimized EPI for fMRI studies of the orbitofrontal cortex. *NeuroImage*, 19(2 Pt 1), 430–441 Available from: <http://www.ncbi.nlm.nih.gov/pubmed/12814592>
- Di Martino, A., Scheres, A., Margulies, D. S., Kelly, A. M. C., Uddin, L. Q., Shehzad, Z., ... Milham, M. P. (2008). Functional connectivity of human striatum: A resting state fMRI study. *Cerebral Cortex*, 18(12), 2735–2747 Available from: <http://www.ncbi.nlm.nih.gov/pubmed/18400794>
- Faraone, S. V. (2018). The pharmacology of amphetamine and methylphenidate: Relevance to the neurobiology of attention-deficit/hyperactivity disorder and other psychiatric comorbidities. *Neuroscience and Biobehavioral Reviews*, 87, 255–270. <https://doi.org/10.1016/j.neubiorev.2018.02.001>
- Flandin, G., & Friston, K. (2008). Statistical parametric mapping (SPM). *Scholarpedia*, 3(4), 6232 Available from: http://www.scholarpedia.org/article/Statistical_parametric_mapping_%28SPM%29
- Flodin, P., Gospic, K., Petrovic, P., & Fransson, P. (2012). Effects of L-dopa and oxazepam on resting-state functional magnetic resonance imaging connectivity: A randomized, cross-sectional placebo study. *Brain Connectivity*, 2(5), 246–253 Available from: <http://www.ncbi.nlm.nih.gov/pubmed/22957904>
- Fong, A. H. C., Yoo, K., Rosenberg, M. D., Zhang, S., Li, C.-S. R., Scheinost, D., ... Chun, M. M. (2019). Dynamic functional connectivity during task performance and rest predicts individual differences in attention across studies. *NeuroImage*, 188, 14–25.
- Fudge, J. L., & Emiliano, A. B. (2003). The extended amygdala and the dopamine system: Another piece of the dopamine puzzle. *The Journal of Neuropsychiatry and Clinical Neurosciences*, 15(3), 306–316.
- Haber, S. N., Kim, K.-S., Maily, P., & Calzavara, R. (2006). Reward-related cortical inputs define a large striatal region in primates that interface with associative cortical connections, providing a substrate for incentive-based learning. *Journal of Neuroscience*, 26(32), 8368–8376. Available from: <http://www.jneurosci.org/content/jneuro/26/32/8368.full.pdf>
- Haber, S. N., & Knutson, B. (2010). The reward circuit: Linking primate anatomy and human imaging. *Neuropsychopharmacology*, 35(1), 4–26 Available from: <http://www.pubmedcentral.nih.gov/articlerender.fcgi?artid=3055449&tool=pmcentrez&rendertype=abstract>
- Hadley, J. A., Nenert, R., Kraguljac, N. V., Bolding, M. S., White, D. M., Skidmore, F. M., ... Lahti, A. C. (2014). Ventral tegmental area/midbrain functional connectivity and response to antipsychotic medication in schizophrenia. *Neuropsychopharmacology*, 39, 1020–1030.
- Hägele, C., Schlagenhaut, F., Rapp, M., Sterzer, P., Beck, A., BERPohl, F., ... Heinz, A. (2015). Dimensional psychiatry: reward dysfunction and depressive mood across psychiatric disorders. *Psychopharmacology (Berl)*, 232(2), 331–341 Available from: <http://www.ncbi.nlm.nih.gov/pubmed/24973896>
- Hass, J., & Durstewitz, D. (2011). Models of dopaminergic modulation. *Scholarpedia*, 6(8), 4215 Available from: http://www.scholarpedia.org/article/Models_of_dopaminergic_modulation
- Hermann, D., Smolka, M. N., Wrase, J., Klein, S., Nikitopoulos, J., Georgi, A., ... Heinz, A. (2006). Blockade of cue-induced brain activation of abstinent alcoholics by a single administration of amisulpride as measured with fMRI. *Alcoholism, Clinical and Experimental Research*, 30(8), 1349–1354 Available from: <http://www.ncbi.nlm.nih.gov/pubmed/16899037>
- Hills, M., & Armitage, P. (1979). The two-period cross-over clinical trial. *British Journal of Clinical Pharmacology*, 8(1), 7–20 Available from:

- <http://www.pubmedcentral.nih.gov/articlerender.fcgi?artid=1429717&tool=pmcentrez&rendertype=abstract>
- Honey, C. J., Sporns, O., Cammoun, L., Gigandet, X., Thiran, J. P., Meuli, R., and Hagmann, P. (2009). Predicting human resting-state functional connectivity from structural connectivity. *Proceedings of the National Academy of Sciences*, 106(6), 2035 Available from: <http://www.pnas.org/content/106/6/2035.abstract>
- Howes, O. D., & Kapur, S. (2009). The dopamine hypothesis of schizophrenia: Version III—the final common pathway. *Schizophrenia Bulletin*, 35(3), 549–562 Available from: <http://www.pubmedcentral.nih.gov/articlerender.fcgi?artid=2669582&tool=pmcentrez&rendertype=abstract>
- Kahnt, T., Weber, S. C., Haker, H., Robbins, T. W., & Tobler, P. N. (2015). Dopamine D2-receptor blockade enhances decoding of prefrontal signals in humans. *The Journal of Neuroscience*, 35(9), 4104–4111 Available from: <http://www.ncbi.nlm.nih.gov/pubmed/25740537>
- Karam, R. G., Rovaris, D. L., Breda, V., Picon, F. A., Victor, M. M., Salgado, C. A. I., ... Bau, C. H. D. (2017). Trajectories of attention-deficit/hyperactivity disorder dimensions in adults. *Acta Psychiatrica Scandinavica*, 136(2), 210–219.
- Kelly, C., de Zubicaray, G., Di Martino, A., Copland, D. A., Reiss, P. T., Klein, D. F., ... McMahon, K. (2009 Jun 3). L-Dopa modulates functional connectivity in striatal cognitive and motor networks: A double-blind placebo-controlled study. *The Journal of Neuroscience*, 29(22), 7364–7378 Available from: <http://www.jneurosci.org/cgi/doi/10.1523/JNEUROSCI.0810-09.2009>
- Kessler, D., Angststadt, M., & Sripada, C. S. (2017). Reevaluating cluster failure; in fMRI using nonparametric control of the false discovery rate. *Proceedings of the National Academy of Sciences of the United States of America*, 114(17), E3372–E3373 Available from: <http://www.ncbi.nlm.nih.gov/pubmed/28420796>
- Kompoliti, K., Adler, C. H., Raman, R., Pincus, J. H., Leibowitz, M. T., Ferry, J. J., ... Goetz, C. G. (2002). Gender and pramipexole effects on levodopa pharmacokinetics and pharmacodynamics. *Neurology*, 58(9), 1418–1422 Available from: <http://www.ncbi.nlm.nih.gov/pubmed/12011296>
- Kriegeskorte, N., Simmons, W. K., Bellgowan, P. S. F., & Baker, C. I. (2009). Circular analysis in systems neuroscience: The dangers of double dipping. *Nature Neuroscience*, 12(5), 535–540 Available from: <http://www.ncbi.nlm.nih.gov/pubmed/19396166>
- la Fougère, C., Meisenzahl, E., Schmitt, G., Stauss, J., Frodl, T., Tatsch, K., ... Dresel, S. (2005). D2 receptor occupancy during high- and low-dose therapy with the atypical antipsychotic amisulpride: A 123I-iodobenzamide SPECT study. *Journal of Nuclear Medicine*, 46(6), 1028–1033 Available from: <http://www.ncbi.nlm.nih.gov/pubmed/15937316>
- Lak, A., Stauffer, W. R., & Schultz, W. (2014). Dopamine prediction error responses integrate subjective value from different reward dimensions. *Proceedings of the National Academy of Sciences*, 111(6), 2343–2348 Available from: <http://www.pnas.org/lookup/doi/10.1073/pnas.1321596111>
- Liu, X., Hairston, J., Schrier, M., & Fan, J. (2011). Common and distinct networks underlying reward valence and processing stages: A meta-analysis of functional neuroimaging studies. *Neuroscience and Biobehavioral Reviews*, 35(5), 1219–1236 Available from: <http://www.pubmedcentral.nih.gov/articlerender.fcgi?artid=3395003&tool=pmcentrez&rendertype=abstract>
- Mark Williams, S., & Goldman-Rakic, P. S. (1998). Widespread origin of the primate mesofrontal dopamine system. *Cerebral Cortex*, 8(4), 321–345.
- Martins, D., Mehta, M. A., & Prata, D. (2017). The “highs and lows” of the human brain on dopaminergics: Evidence from neuropharmacology. *Neuroscience & Biobehavioral Reviews*, 80, 351–371. Available from: <https://doi.org/10.1016/j.neubiorev.2017.06.003>
- Menon, V. (2015). Salience network. In A. W. Toga (Ed.), *Brain mapping: An encyclopedic reference* (pp. 597–611). Elsevier Inc. Available from: <https://doi.org/10.1016/B978-0-12-397025-1.00052-X>
- Metzger, C. D., Wieggers, M., Walter, M., Abler, B., & Graf, H. (2015). Local and global resting state activity in the noradrenergic and dopaminergic pathway modulated by reboxetine and amisulpride in healthy subjects. *The International Journal of Neuropsychopharmacology*, 19(2), pyv080. <https://doi.org/10.1093/ijnp/pyv080>
- Mobbs, D., Trimmer, P. C., Blumstein, D. T., & Dayan, P. (2018). Foraging for foundations in decision neuroscience: insights from ethology. *Nature Reviews Neuroscience*, 1, 419–427. Available from: <http://www.nature.com/articles/s41583-018-0010-7>
- Muthuraman, M., Koirala, N., Ciolac, D., Pinteá, B., Glaser, M., Groppa, S., ... Groppa, S. (2018). Deep brain stimulation and L-DOPA therapy: Concepts of action and clinical applications in Parkinson's disease. *Frontiers in Neurology*, 9, 711 Available from: <https://www.frontiersin.org/article/10.3389/fneur.2018.00711/full>
- Nigg, J. T. (2017). Annual research review: On the relations among self-regulation, self-control, executive functioning, effortful control, cognitive control, impulsivity, risk-taking, and inhibition for developmental psychopathology. *The Journal of Child Psychology and Psychiatry and Allied Disciplines*, 58, 361–383.
- Pauli, W. M., Nili, A. N., & Tyszka, J. M. (2018). A high-resolution probabilistic in vivo atlas of human subcortical brain nuclei. *Scientific Data*, 5, 180063 Available from: <http://www.nature.com/articles/sdata201863>
- Pauli, W. M., O'Reilly, R. C., Yarkoni, T., & Wager, T. D. (2016). Regional specialization within the human striatum for diverse psychological functions. *Proceedings of the National Academy of Sciences*, 113(7), 1907–1912 Available from: <http://www.pnas.org/lookup/doi/10.1073/pnas.1507610113>
- Piray, P., den Ouden, H. E. M., van der Schaaf, M. E., Toni, I., & Cools, R. (2017). Dopaminergic modulation of the functional ventrodorsal architecture of the human striatum. *Cerebral Cortex*, 27(1), 485–495.
- Plichta, M. M., & Scheres, A. (2014). Ventral-striatal responsiveness during reward anticipation in ADHD and its relation to trait impulsivity in the healthy population: A meta-analytic review of the fMRI literature. *Neuroscience and Biobehavioral Reviews*, 38, 125–134 Available from: <http://www.ncbi.nlm.nih.gov/pubmed/23928090>
- Power, J. D., Barnes, K. A., Snyder, A. Z., Schlaggar, B. L., & Petersen, S. E. (2012). Spurious but systematic correlations in functional connectivity MRI networks arise from subject motion. *NeuroImage*, 59(3), 2142–2154 Available from: <http://www.ncbi.nlm.nih.gov/pubmed/22019881>
- Rosenzweig, P., Canal, M., Patat, A., Bergougnan, L., Zieleniuk, I., & Bianchetti, G. (2002 Jan). A review of the pharmacokinetics, tolerability and pharmacodynamics of amisulpride in healthy volunteers. *Human Psychopharmacology*, 17(1), 1–13 Available from: <http://www.ncbi.nlm.nih.gov/pubmed/12404702>
- Rubia, K. (2011). “Cool” inferior frontostriatal dysfunction in attention-deficit/hyperactivity disorder versus “hot” ventromedial orbitofrontal- limbic dysfunction in conduct disorder: A review. *Biological Psychiatry*, 69(12), e69–e87 Available from: <https://www.sciencedirect.com/science/article/pii/S0006322310009881>
- Rubia, K., Halari, R., Christakou, A., & Taylor, E. (2009). Impulsiveness as a timing disturbance: Neurocognitive abnormalities in attention-deficit hyperactivity disorder during temporal processes and normalization with methylphenidate. *Philosophical Transactions of the Royal Society of London. Series B, Biological Sciences*, 364(1525), 1919–1931 Available from: <http://www.ncbi.nlm.nih.gov/pubmed/19487194>
- Rubia, K., Halari, R., Cubillo, A., Mohammad, A.-M., Brammer, M., & Taylor, E. (2009). Methylphenidate normalises activation and functional connectivity deficits in attention and motivation networks in medication-naïve children with ADHD during a rewarded continuous performance task. *Neuropharmacology*, 57(7–8), 640–652.
- Schmidt, R. E., Gay, P., D'Acremont, M., & Van Der Linden, M. (2008). A German adaptation of the upps impulsive behavior scale: Psychometric properties and factor structure. *Swiss Journal of Psychology*, 67, 107–112.

- Schoemaker, H., Claustre, Y., Fage, D., Rouquier, L., Chergui, K., Curet, O., ... Scatton, B. (1997). Neurochemical characteristics of amisulpride, an atypical dopamine D2/D3 receptor antagonist with both presynaptic and limbic selectivity. *The Journal of Pharmacology and Experimental Therapeutics*, 280(1), 83–97 Available from: <http://www.ncbi.nlm.nih.gov/pubmed/8996185>
- Schultz, W. (2015). Neuronal reward and decision signals: From theories to data. *Physiological Reviews*, 95(3), 853–951 Available from: <http://www.ncbi.nlm.nih.gov/pubmed/26109341>
- Shin, L., & Bush, G. (2011). Exaggerated activation of dorsal anterior cingulate cortex during cognitive interference: A monozygotic twin study of posttraumatic stress disorder. *American Journal of Psychiatry*, 168, 979–985. Available from: <http://www.cme.psychiatryonline.org/article.aspx?articleid=116564&RelatedWidgetArticles=true>
- Shirer, W. R., Ryali, S., Rykhlevskaia, E., Menon, V., & Greicius, M. D. (2012). Decoding subject-driven cognitive states with whole-brain connectivity patterns. *Cerebral Cortex*, 22(1), 158–165.
- Stice, E., Yokum, S., Bohon, C., Marti, N., & Smolen, A. (2010). Reward circuitry responsivity to food predicts future increases in body mass: Moderating effects of DRD2 and DRD4. *NeuroImage*, 50(4), 1618–1625 Available from: <http://www.pubmedcentral.nih.gov/articlerender.fcgi?artid=3987805&tool=pmcentrez&rendertype=abstract>
- Ströhle, A., Stoy, M., Wrase, J., Schwarzer, S., Schlagenhauf, F., Huss, M., ... Heinz, A. (2008). Reward anticipation and outcomes in adult males with attention-deficit/hyperactivity disorder. *NeuroImage*, 39(3) 966–972. <http://www.mendeley.com/research/reward-anticipation-outcomes-adult-males-attentiondeficithyperactivity-disorder>
- Tomasi, D., & Volkow, N. D. (2014). Functional connectivity of substantia nigra and ventral tegmental area: Maturation during adolescence and effects of ADHD. *Cerebral Cortex*, 24, 935–944.
- Urry, H. L., van Reekum, C. M., Johnstone, T., Kalin, N. H., Thurow, M. E., Schaefer, H. S., ... Davidson, R. J. (2006). Amygdala and ventromedial prefrontal cortex are inversely coupled during regulation of negative affect and predict the diurnal pattern of cortisol secretion among older adults. *The Journal of Neuroscience*, 26(16), 4415–4425 Available from: <http://www.jneurosci.org/cgi/content/abstract/26/16/4415>
- Vogt, B. A. (2016). Midcingulate cortex: Structure, connections, homologues, functions and diseases. *Journal of Chemical Neuroanatomy*, 74, 28–46. <https://doi.org/10.1016/j.jchemneu.2016.01.010>
- Von Rhein, D., Mennes, M., van Ewijk, H., Groenman, A. P., Zwiers, M. P., Oosterlaan, J., ... Buitelaar, J. (2015). The NeuroIMAGE study: A prospective phenotypic, cognitive, genetic and MRI study in children with attention-deficit/hyperactivity disorder. Design and descriptives. *European Child & Adolescent Psychiatry*, 24(3), 265–281.
- Vuilleumier, P., Richardson, M. P., Armony, J. L., Driver, J., & Dolan, R. J. (2004). Distant influences of amygdala lesion on visual cortical activation during emotional face processing. *Nature Neuroscience*, 7(11), 1271–1278. <https://doi.org/10.1038/nn1341>
- Vul, E., & Pashler, H. (2017). Suspiciously high correlations in brain imaging research. In *Psychological science under scrutiny: Recent Challenges and Proposed Solutions*, S. O. Lilienfeld & I. D. Waldman (Eds.), <https://doi.org/10.1002/9781119095910.ch11>
- Wellek, S., & Blettner, M. (2012). On the proper use of the crossover design in clinical trials: Part 18 of a series on evaluation of scientific publications. *Deutsches Ärzteblatt International*, 109(15), 276–281 Available from: <http://www.pubmedcentral.nih.gov/articlerender.fcgi?artid=3345345&tool=pmcentrez&rendertype=abstract>
- Westerink, B. H. C., & Korf, J. (1976). Comparison of effects of drugs on dopamine metabolism in the substantia nigra and the corpus striatum of rat brain. *European Journal of Pharmacology*, 40(1), 131–136 Available from: <https://www.sciencedirect.com/science/article/pii/0014299976903629?via%3Dihub>
- Whiteside, S. P., & Lynam, D. R. (2003). Understanding the role of impulsivity and externalizing psychopathology in alcohol abuse: Application of the UPPS impulsive behavior scale. *Experimental and Clinical Psychopharmacology*, 11, 210–217.
- Whitfield-Gabrieli, S. (2012). Nieto-Castanon a. Conn: A functional connectivity toolbox for correlated and anticorrelated brain networks. *Brain Connectivity*, 2(3), 125–141 Available from: <http://online.liebertpub.com/doi/abs/10.1089/brain.2012.0073>
- Whitton, A. E., Treadway, M. T., & Pizzagalli, D. A. (2015). Reward processing dysfunction in major depression, bipolar disorder and schizophrenia. *Current Opinion in Psychiatry*, 28(1), 7–12.

SUPPORTING INFORMATION

Additional supporting information may be found online in the Supporting Information section at the end of this article.

How to cite this article: Grimm O, Kopfer V, Küpper-Tetzl L, et al. Amisulpride and L-DOPA modulate subcortical brain nuclei connectivity in resting-state pharmacologic magnetic resonance imaging. *Hum Brain Mapp*. 2020;41:1806–1818. <https://doi.org/10.1002/hbm.24913>